Engineering and Technology Journal e-ISSN: 2456-3358
Volume 11 Issue 09 September -2026, Page No.- 11543- 11548
DOI: 10.47191/etj/v11i09.18, I.F. – 8.595
© 2026, ETJ

# Harmonic Performance Assessment of a Fuzzy Controlled Grid Connected Photovoltaic Battery System

**Alele Jude O[1], Eyenubo O. J[2], Emmanuel E. Obuseh[3], Ezekiel Ebimene E[4], Jeffery U. Okieke[5], Anamonye Gabriel U[6]**
[1,2,3,4,5,6] Department of Electrical/Electronic Engineering, Delta State University, Oleh Campus, Delta State, Nigeria.

**ABSTRACT:** This study assesses the voltage harmonic performance of a fuzzy controlled grid connected photovoltaic–battery system using harmonic results reported from a MATLAB/Simulink model. The analysis concentrates on the third, fifth, seventh and ninth harmonics and on the consistency of the reported total harmonic distortion (THD). The listed harmonic magnitudes decreased from 2.85%, 3.60%, 2.10% and 1.25% without fuzzy control to 1.20%, 1.85%, 1.10% and 0.65% with fuzzy control, respectively. Relative reductions ranged from 47.62% to 57.89%. The fifth harmonic remained the largest listed component, although its magnitude fell by 1.75 percentage points. Reported voltage THD decreased from 7.85% to 3.42%, corresponding to a 56.43% relative reduction. However, root-sum-square reconstruction from the four specified orders yielded 5.20% and 2.55%, respectively. Including the separately reported higher-order entry as an aggregate increased these estimates to 5.32% and 2.59%, leaving the reported totals unreconciled. The available evidence therefore indicates lower listed voltage harmonics with fuzzy control but does not establish a complete spectrum or standards compliance. The contribution is a focused comparison of harmonic attenuation and a transparent assessment of the spectral information required to substantiate aggregate performance.

**KEYWORDS:** Photovoltaic System; Battery Storage; Fuzzy Logic Control; Voltage Harmonics; Total Harmonic Distortion; Power Quality.

## 1.0 INTRODUCTION

As photovoltaic (PV) deployment expands, the quality of converter-mediated electrical supply becomes an essential integration issue (IEA Photovoltaic Power Systems Programme, 2026). Renewable generation also operates within wider sustainability constraints: decarbonization depends on policy and regional implementation (Obuseh et al., 2025), while PV life-cycle impacts extend across production, operation and end-of-life management (Obuseh et al., 2026). Harmonic assessment addresses the electrical interface within this broader context.

In Nigerian power systems, distribution constraints and generation reliability provide a practical motivation for improved control. Studies of the Oria Abraka substation and a Southern Nigerian thermal station examined supply adequacy and equipment reliability, respectively (Eyenubo et al., 2025). Local ANN–PSO load forecasting and industrial telemetry studies further illustrate the roles of prediction and measurement in operational decision-making (Eyenubo et al., 2025; Otuagoma et al., 2025). These contextual studies do not directly validate harmonic mitigation in a PV inverter.

PV inverter control serves several distinct purposes. Smart-inverter active-power functions have been investigated for network voltage and frequency support (Howlader et al., 2020), while hybrid maximum-power-point tracking has been studied under changing atmospheric conditions (Zaghba et al., 2024). Power extraction and network support can influence converter operation, but successful regulation of those quantities do not by itself quantify waveform distortion. Harmonic magnitudes require an explicit spectral assessment.

Fuzzy logic provides a rule-based means of handling nonlinear operating relationships. Assem et al. (2023) investigated adaptive fuzzy control and management of PV systems with battery storage, and Bahri et al. (2025) applied fuzzy regulation to a three-level boost converter for DC-voltage control. At the scheduling level, fuzzy-controlled hybrid storage has been studied under time-of-use tariffs (Shirinda et al., 2024), while predictive and adaptive fuzzy methods have been applied to microgrid energy management (Cavus et al., 2025). These studies establish relevant control contexts, while also showing why energy-management outcomes and harmonic outcomes should be assessed separately.

Power-quality applications place greater emphasis on the converter, compensation strategy and measurement point. Ravi et al. (2023) examined fuzzy control of an interline unified power-quality conditioner. El Sayed et al. (2024) combined fuzzy control and optimization in a grid-connected PV/wind system addressing fault ride-through and power quality. Both studies concern architectures with additional functions, so their outcomes cannot be transferred directly to a PV–battery supervisory controller.

Recent work has also investigated optimized inverter regulation. Mohamed et al. (2025) evaluated hybrid fuzzy–PI control with metaheuristic tuning for a large PV plant, whereas Gupta et al. (2025) investigated Grey Wolf optimization of PID control. Boopathi and Indragandhi (2025) studied predictive direct-power control of a PV-interfaced multilevel shunt active filter, with simulation and experimental assessment. These alternatives reinforce the need to specify the baseline controller, filter and operating conditions before attributing a distortion reduction to any one control strategy.

For systems containing storage, Abbasi et al. (2025) examined source and filter coordination under nonlinear loading. Govil et al. (2025) assessed PV-DSTATCOM operation through real-time simulation under balanced and unbalanced conditions. Together, these studies show that source operating mode, compensation hardware and test conditions form part of the power-quality result. A single percentage cannot fully describe those dependencies. IEEE 519-2022 provides a framework for harmonic control in electric power systems; assessment against it requires the appropriate measurement location and applicable conditions (IEEE, 2022).

The present study addresses a narrower question: how do the individually reported low-order voltage harmonics change between the cases without and with fuzzy control, and how well do those components support the reported THD totals? The objectives are to quantify absolute and relative attenuation, identify the dominant remaining listed order, and reconstruct distortion from the available component magnitudes. The contribution is a focused harmonic assessment of an existing simulation case, including explicit spectral consistency checks. It does not introduce a new converter topology or a newly optimized fuzzy controller.

## 2.0 MATERIALS AND METHODS

### 2.1 System and source data

The analysis uses the harmonic table in Chapter Four of the underlying dissertation. The source model was developed in MATLAB/Simulink and comprises a PV array, boost converter, battery with a bidirectional DC–DC converter, DC link, three-phase voltage-source inverter, output filter and utility connection. A phase-locked loop provides synchronization. Table 1 summarizes the declared electrical configuration relevant to interpreting the harmonic results.

**Table 1. Declared simulation configuration**

| Quantity | Reported setting |
| --- | --- |
| Grid voltage | 400 V line-to-line RMS |
| Fundamental frequency | 50 Hz |
| DC-link reference | 700 V |
| Switching frequency | 10 kHz |
| PV rated power | 100 kW |
| Battery capacity | 200 kWh |
| Filter inductance | 2–5 mH |
| Filter capacitance | 10–20 µF |

The configuration table is retained as source information. The source alternates between LC and LCL filter descriptions and does not identify unique component values within the listed ranges. The harmonic operating power, load composition, grid impedance and battery mode are not explicitly linked to the reported spectrum. Consequently, the declared ratings do not establish the exact operating point of the harmonic comparison.

### 2.2 Fuzzy control context

The model describes Mamdani fuzzy inference using an error and its change as inputs. Five linguistic levels partition the normalized interval from −1 to 1: negative big, negative small, zero, positive small and positive big. A 25-rule matrix maps each input pair to an output level, followed by centroid defuzzification. The voltage channel provides a reactive-power correction; a separate active-power channel is part of the wider system. Only the reported harmonic outcomes are evaluated here.

The physical input and output gains, exact membership breakpoints, command limits and controller sampling interval are not completely specified. The source also contains conflicting error-sign descriptions. The analysis therefore preserves the original comparison labels, "without fuzzy control" and "with fuzzy control," without treating the baseline as a fully documented PI benchmark. Reduced harmonics may be associated with the overall controlled converter response; the available data do not isolate a harmonic-selective action of the fuzzy rules.

### 2.3 Harmonic metrics

The source expresses the harmonic entries as percentages. They are interpreted as magnitudes relative to the fundamental of the same voltage quantity. Equation (1) defines the normalized harmonic magnitude, where Vh and V1 denote the RMS harmonic and fundamental amplitudes.

$$a_h = \frac{V_h}{V_1} \times 100 \quad (1)$$

For a finite spectrum ending at order H, voltage THD is defined by Equation (2). The upper order must be specified when comparing independently produced spectra.

$$THD_v = \frac{\sqrt{\sum_{h=2}^{H} V_h{}^2}}{V_1} \times 100\% \quad (2)$$

For each listed order, absolute attenuation Δah is the baseline magnitude minus the controlled magnitude, expressed in percentage points. Relative attenuation Rh is given by Equation (3), where subscripts 0 and F designate the baseline and fuzzy-controlled cases.

$$R_h = \frac{a_{h,0} - a_{h,F}}{a_{h,0}} \times 100\% \quad (3)$$

The same relative-change calculation is applied to the two reported THD totals. To check spectral consistency, the root-sum-square magnitude D4 of only the four individually specified orders is calculated using Equation (4). This is a partial-spectrum indicator, not a replacement for full THD.

$$D_4 = \sqrt{a_3{}^2 + a_5{}^2 + a_7{}^2 + a_9{}^2} \quad (4)$$

The separately tabulated "higher-order harmonics" entry has no stated order range or aggregation rule. A conditional second check treats this entry as the root-sum-square aggregate of all remaining orders. Under that assumption, the reconstructed distortion DA is given by Equation (5), where aHO is the higher-order entry.

$$D_A = \sqrt{D_4{}^2 + a_{HO}{}^2} \quad (5)$$

All derived values use the supplied two-decimal magnitudes without intermediate rounding. No additional simulation, reconstructed time waveform or inferred FFT spectrum is presented as an observation. Independent repeated runs and raw samples were unavailable; therefore confidence intervals and statistical significance tests are not reported.

## 3.0 RESULTS AND DISCUSSION

### 3.1 Individual voltage harmonics

Table 2 presents the reported component magnitudes and the corresponding calculated attenuation. At the nominal 50 Hz fundamental, the selected orders occur at 150, 250, 350 and 450 Hz. Figure 1 displays their paired magnitudes to make the change in the spectrum easier to compare.

**Table 2. Reported magnitudes and calculated attenuation**

| Order | Without (%) | With (%) | Drop (pp) | Drop (%) |
|---|---|---|---|---|
| 3 | 2.85 | 1.20 | 1.65 | 57.89 |
| 5 | 3.60 | 1.85 | 1.75 | 48.61 |
| 7 | 2.10 | 1.10 | 1.00 | 47.62 |
| 9 | 1.25 | 0.65 | 0.60 | 48.00 |

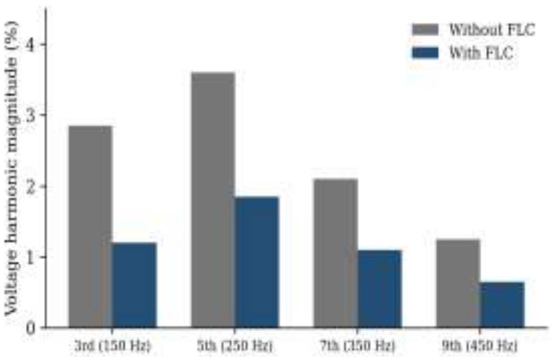


**Figure 1. Listed voltage harmonics without and with fuzzy control; redrawn from the source table.**

Every listed magnitude is smaller in the fuzzy-controlled case. The fifth harmonic has the largest absolute decrease, falling by 1.75 percentage points from 3.60% to 1.85%. The third harmonic decreases by 1.65 percentage points, while the seventh and ninth decrease by 1.00 and 0.60 percentage points, respectively. These reductions refer to normalized voltage magnitudes; absolute harmonic voltages cannot be calculated reliably without the fundamental amplitude used for each spectrum.

### 3.2 Relative attenuation and remaining distortion

Figure 2 compares the calculated relative attenuation. The third harmonic exhibits the greatest proportional reduction, at 57.89%. The fifth, seventh and ninth decrease by 48.61%, 47.62% and 48.00%, respectively. Thus, the largest initial component and the greatest proportional improvement occur at different orders.

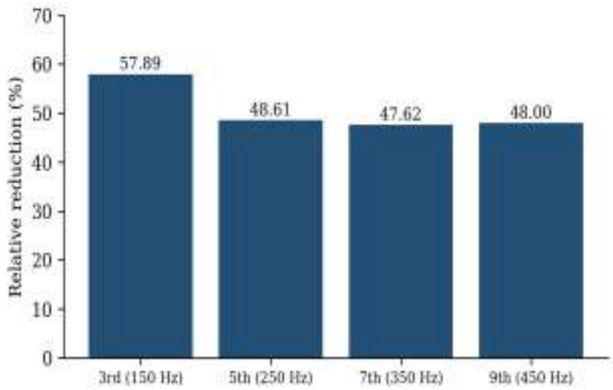


**Figure 2. Relative attenuation calculated separately for each listed harmonic order.**

The fifth harmonic remains the largest listed component after control. Its squared magnitude represents 47.90% of the squared four-order total before control and 52.69% after control. These shares describe the selected subset only. They identify the fifth harmonic as a useful target for subsequent controller and filter investigation, but do not establish that it dominates the complete spectrum. The increased share occurs because the other selected components collectively decrease more strongly relative to their initial contribution.

The reduction in third and ninth components should also be interpreted with care because the source does not unambiguously identify the measured voltage as phase-to-neutral or line-to-line. The harmonic table alone cannot resolve that measurement convention or the corresponding network topology. Confirmation of the signal definition is necessary before drawing conclusions about three-phase harmonic propagation.

### 3.3 Reported THD and reconstruction

The reported voltage THD decreases by 4.43 percentage points, from 7.85% to 3.42%. This corresponds to a relative reduction of 56.43%. Table 3 compares those totals with values calculated from the listed spectrum. Figure 3 illustrates the remaining gap between the reported and reconstructed indicators.

**Table 3. Aggregate distortion and spectral consistency**

| Indicator | Without (%) | With (%) |
|---|---|---|
| Reported THD | 7.85 | 3.42 |
| Four-order RSS, D4 | 5.20 | 2.55 |
| Higher-order entry | 1.10 | 0.45 |
| Conditional RSS, DA | 5.32 | 2.59 |

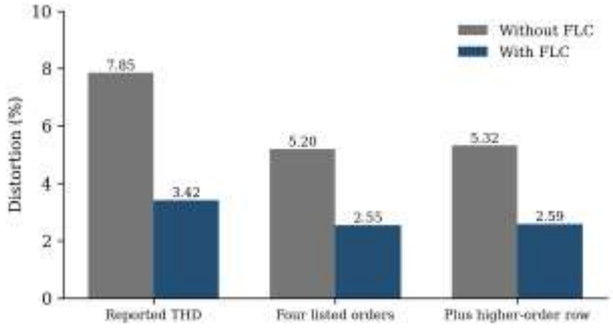


**Figure 3. Reported THD compared with partial and conditional spectral reconstructions. The higher-order aggregation is an assumption.**

The four-order calculation gives 5.20% without fuzzy control and 2.55% with fuzzy control, a relative decrease of 51.00%. Treating the higher-order entry as an aggregate gives 5.32% and 2.59%, respectively. Neither pair reproduces the reported THD totals. The mismatch does not reverse the attenuation observed in the listed components, but it prevents verification of the reported full-spectrum reduction from the available table.

Possible explanations include omitted orders, different FFT windows, different voltage signals or an alternative meaning of the higher-order entry. The source record does not distinguish among these possibilities. The THD totals are therefore retained as reported values rather than silently replaced with partial-spectrum estimates. Correcting the totals requires the original signal export or a complete harmonic report from the same operating point.

### 3.4 Interpretation against related studies

The observed direction of change is compatible with research on fuzzy and optimized converter regulation, including the fuzzy–PI investigation by Mohamed et al. (2025) and the fuzzy conditioner study by Ravi et al. (2023). Compatibility in direction is not proof of equal control mechanisms. In those systems, controller tuning, converter topology and compensation functions differ from the present supervisory arrangement.

Studies using dedicated filtering or compensation also have different evaluation boundaries. Boopathi and Indragandhi (2025) explicitly consider a multilevel shunt active filter, while Abbasi et al. (2025) vary source and filter combinations. Govil et al. (2025) use real-time simulation to assess PV-DSTATCOM operation. Their results should not be ranked against the present voltage THD solely by comparing headline percentages, because the measured quantities, operating conditions and validation methods are not matched.

A standards-compliance conclusion is also unsupported by the available information. IEEE 519-2022 addresses harmonic control with requirements tied to the appropriate point of assessment (IEEE, 2022). The source does not establish that the tabulated inverter voltage is a documented PCC measurement, nor does it report a complete spectrum and compatible evaluation interval. Accordingly, 3.42% is treated as a reported simulation indicator, without a claim of verified IEEE compliance.

### 3.5 Limitations and reproducibility

The principal limitation is the absence of raw voltage data linking both cases to an identical measurement point, load, irradiance, filter and FFT configuration. The supplied results provide one paired set of rounded harmonic magnitudes. They do not demonstrate performance across operating conditions, sensitivity to grid impedance or robustness to controller parameter changes. Battery participation in harmonic improvement is likewise not isolated by a separate comparison.

A reproducible follow-up should export the same voltage quantity for both controller states after a specified settling interval, report the fundamental amplitude, FFT window, sampling rate and maximum included order, and reconcile every component with its THD total. The model should also identify the actual filter, controller gains and baseline settings. Matched nonlinear-load cases and hardware or real-time validation would strengthen the interpretation. These are proposed validation steps, not tests completed in this study.

## 4.0 CONCLUSION

The focused comparison shows lower third, fifth, seventh and ninth voltage harmonic magnitudes in the fuzzy-controlled case. Relative attenuation ranges from 47.62% to 57.89%, and the fifth harmonic remains the largest listed component despite a 1.75-percentage-point decrease. Reported THD falls from 7.85% to 3.42%, but spectral reconstruction yields smaller totals and exposes an unresolved inconsistency in the aggregate record. The supported conclusion is that the listed harmonics improve under the reported controlled condition. Full-spectrum performance, causal attribution to the fuzzy controller and standards compliance require reconciled source data and matched validation. The order-by-order assessment identifies a clear basis for that subsequent work.

**REFERENCES**


1. Abbasi, M. S. W., Kazmi, S. A. A., Billah, M., Altamimi, A., Khan, Z. A., & Alghassab, M. (2025). Power quality optimization framework for three phase microgrids with grid tied solar PV and battery storage under nonlinear loads. Scientific Reports, 15, Article 42568. https://doi.org/10.1038/s41598-025-18954-3
2. Assem, H., Azib, T., Bouchafaa, F., Laarouci, C., Belhaouas, N., & Hadj Arab, A. (2023). Adaptive fuzzy logic-based control and management of photovoltaic systems with battery storage. International Transactions on Electrical Energy Systems, 2023, Article 9065061. https://doi.org/10.1155/2023/9065061
3. Bahri, A., Benamrane, K., Abdelkrim, T., Bechouat, M., Mezhoud, N., & Ayachi, B. (2025). Three-level boost converter with fuzzy logic for PV-battery energy systems in DC voltage control. Journal Européen des Systèmes Automatisés, 58(1), 1–12. https://doi.org/10.18280/jesa.580101
4. Boopathi, R., & Indragandhi, V. (2025). Enhancement of power quality in grid-connected systems using a predictive direct power controlled based PV-interfaced with multilevel inverter shunt active power filter. Scientific Reports, 15, Article 7967. https://doi.org/10.1038/s41598-025-92693-3
5. Cavus, M., Dissanayake, D., & Bell, M. C. (2025). Deep-fuzzy logic control for optimal energy management: A predictive and adaptive framework for grid-connected microgrids. Energies, 18(4), Article 995. https://doi.org/10.3390/en18040995
6. El Sayed, N. G., Yousef, A. M., El-Saady, G., Alanazi, M. D., Ziedan, H. A., & Abdelsattar, M. (2024). Artificial intelligent fuzzy control and LAPO algorithm for enhancement LVRT and power quality of grid connected PV/wind hybrid systems. Scientific Reports, 14, Article 30475. https://doi.org/10.1038/s41598-024-78384-5
7. Eyenubo, O. J., Obuseh, E. E., Ebisine, E. E., Okieke, U. J., Otuagoma, S. O., & Urhefe, O. V. (2025). Hybrid ANN-PSO model for short-term electricity load forecasting: A case study of Oleh power system. NIPES Journal of Science and Technology Research, 7(4), 1–17. https://doi.org/10.37933/nipes/7.4.2025.1454
8. Eyenubo, O. J., Obuseh, E. E., Ebisine, E. E., Okpare, A. O., & Okieke, U. J. (2025). Analysis of Oria Abraka 33/11 kV power sub-station: A case for sustainable power supply. NIPES Journal of Science and Technology Research, 7(1), 204–218. https://doi.org/10.37933/nipes/7.1.2025.17
9. Govil, V. K., Tripathi, S. M., & Sahay, K. (2025). Real-time assessment of PV-DSTATCOM for grid power quality enhancement using an indirect current control strategy. Scientific Reports, 15, Article 19516. https://doi.org/10.1038/s41598-025-01078-z
10. Gupta, M., Tiwari, P. M., Viral, R. K., Shrivastava, A., Abu Zneid, B., & Hunko, I. (2025). Grid-connected PV inverter system control optimization using Grey Wolf optimized PID controller. Scientific Reports, 15, Article 28869. https://doi.org/10.1038/s41598-025-10617-7
11. Howlader, A. M., Sadoyama, S., Roose, L. R., & Chen, Y. (2020). Active power control to mitigate voltage and frequency deviations for the smart grid using smart PV inverters. Applied Energy, 258, Article 114000. https://doi.org/10.1016/j.apenergy.2019.114000
12. IEA Photovoltaic Power Systems Programme. (2026). Snapshot of global PV markets 2026. https://iea-pvps.org/snapshot-reports/snapshot-2026/
13. IEEE. (2022). IEEE standard for harmonic control in electric power systems (IEEE Std 519-2022). https://standards.ieee.org/ieee/519/10677/
14. Mohamed, M. A. E., Ward, S. A., El-Gohary, M. F., & Mohamed, M. A. (2025). Hybrid fuzzy logic–PI control with metaheuristic optimization for enhanced performance of high-penetration grid-connected PV systems. Scientific Reports, 15, Article 24650. https://doi.org/10.1038/s41598-025-09336-w
15. Obuseh, E. E., Ebisine, E. E., Okieke, J. U., Aloamaka, C. A., & Anamonye, G. U. (2025). Sustainability of decarbonization: A systematic review of policy integration and regional realities. Nigerian Journal of Sustainability Research, 3(2), 77–95. https://njsr.com.ng/index.php/home/article/view/49
16. Obuseh, E. E., Otuagoma, S. O., Ilori, E. G., Anamonye, U. G., Okieke, U. J., & Eyenubo, O. J. (2026). Sustainability of solar photovoltaic systems: A life cycle assessment review. Nigerian Journal of Sustainability Research, 4(1), 387–410. https://njsr.com.ng/index.php/home/article/view/70
17. Ogbah, G. O., Ubeku, E. U., Otuagoma, S. O., Eyenubo, J. O., & Obuseh, E. E. (2025). Reliability evaluation of thermal power stations: A case study of a power station in Southern Nigeria. Journal of Engineering Research Innovation and Scientific Development, 3(3), 29–33. https://doi.org/10.61448/jerisd33256
18. Otuagoma, S. O., Obuseh, E. E., Oyubu, A. O., Okpare, A., Eyenubo, O. J., & Tanen, B. R. (2025). Assessment of conveyor telemetry system in a manufacturing firm: A case study of a brewery in Eastern Nigeria. NIPES Journal of Science and Technology Research, 7(2), 44–58. https://doi.org/10.37933/nipes/7.2.2025.3

19. Ravi, T., Kumar, K. S., Dhanamjayulu, C., Khan, B., & Rajalakshmi, K. (2023). Analysis and mitigation of PQ disturbances in grid connected system using fuzzy logic based IUPQC. Scientific Reports, 13, Article 22425. https://doi.org/10.1038/s41598-023-49042-z
20. Shirinda, K., Kusakana, K., & Ostraszewski, M. (2024). Combinatorial optimization of a fuzzy logic-controlled grid connected photovoltaic with hybrid energy storage systems using time of use tariff. Journal of Energy Storage, 99, Article 113251. https://doi.org/10.1016/j.est.2024.113251
21. Zaghba, L., Borni, A., Khennane Benbitour, M., Fezzani, A., Alwabli, A., Bajaj, M., Dost Mohammadi, S. A., & Ghoneim, S. S. M. (2024). Enhancing grid-connected photovoltaic system performance with novel hybrid MPPT technique in variable atmospheric conditions. Scientific Reports, 14, Article 8205. https://doi.org/10.1038/s41598-024-59024-4